Sensor systems

Flexible Sensor and Readout Circuitry for Continuous Ion Sensing in Sweat

Mattia Petrelli[1*], Ata Golparvar[2], Ali Meimandi[2*], Bajramshahe Shkodra[1], Martina Aurora Costa Angeli[1**], Aniello Falco[1], Paolo Lugli[1***], Luisa Petti[1†], and Sandro Carrara[2***]

[1] *Sensing Technologies Laboratory (STL), Faculty of Engineering, Free University of Bozen-Bolzano, 39100 Bozen, Italy*
[2] *Bio/CMOS Interfaces Laboratory (BCI), École Polytechnique Fédérale de Lausanne (EPFL), 2000 Neuchatel, Switzerland*
[*] *Graduate Student Member, IEEE*
[**] *Member, IEEE*
[***] *Fellow, IEEE*
[†] *Senior Member, IEEE*

Manuscript received 2 May 2023; revised 5 May 2023; accepted 6 May 2023. Date of publication 9 May 2023; date of current version 23 May 2023.

Abstract—In this letter, we present a custom-designed and flexible readout circuitry for the characterization of flexible and planar electrolyte-gated carbon nanotube field-effect transistor-based biosensors for ammonium detection in sweat. We employed spray-deposited semiconducting carbon nanotubes as active material, and functionalized the devices with previously synthesized ion-selective membrane, based on the nonactin ionophore. In the design of the readout circuitry, we focused on enabling low-power operation with a single coin-cell battery with compact wireless data transmission. To maximize the bendability of the flexible PCB, particular attention was taken in layout routing as well as in selecting small-sized packages for the commercial integrated circuits and all-in-one systems such as programmable Bluetooth system-on-chip (i.e., ST microelectronics BlueNRG SoC). We recorded a high sensitivity of 4.516 μA/decade for sweat ammonium level analysis between 0.1 and 100 mM, which fully covers the relevant range of interest in the context of sport monitoring. The characterization was carried out with the introduced front-end readout, and the results were benchmarked with a "gold standard" instrument, showing good and reliable performance of the developed fully flexible bioelectronic system.

Index Terms—Sensor systems, biosensors, carbon nanotubes, electrolyte-gated transistors, flexible sensor readout, soft/flexible electronics, sweat analysis, U-shaped gate.

I. INTRODUCTION

Wearable technology has demonstrated a tremendous breakthrough in the last decade by enabling continuous monitoring of the physiological status [1], [2]. In particular, sweat analysis has opened new pathways in understanding the body's biochemistry, as it represents an optimal candidate to replace the conventional and invasive blood biosensing [3]. Sweat, in fact, is easily accessible from the skin, and enables the extraction of a significant amount of information, being rich in biological indicators [4], [5].

Among the various biological indicators present in sweat, ammonium (NH_4^+) has recently been recognized as an important parameter in the context of sport science [6], as an up-and-coming key biomarker for the metabolic breakdown of proteins, especially in the physiological concentrations (0.12–2.17 mM) [7]. The most widespread methodology for the biosensing of NH_4^+ in sweat is based on electrochemical sensors [8], [9]. Electrolyte-gated field-effect transistors (EG-FETs) represent a promising alternative sensing platform [10], [11]. In particular, carbon nanotube (CNT)-based EG-FETs (EG-CNTFETs) enable the exploitation of the favorable properties of CNTs for the fabrication of highly sensitive biosensing platforms [12], [13]. Moreover, EG-CNTFETs can be easily integrated onto flexible polymeric foils including, among the others, polyimide (PI) and polyethylene terephthalate (PET) [14], [15]. Such flexible substrates enable the integration of sensors in wearable platforms of arbitrary shape, with the possibility of meeting the requirements (e.g., low-cost, large area, flexibility, and conformability) needed to achieve proper market penetration [16].

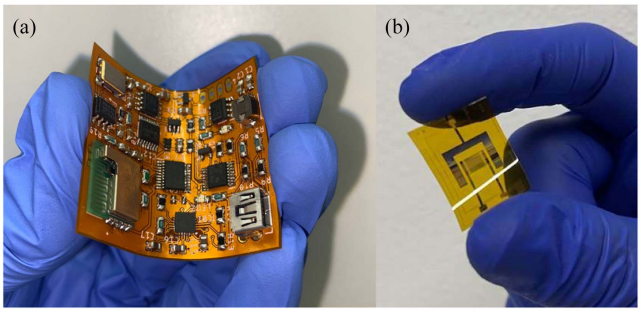

Fig. 1. (a) Proposed flexible front-end readout circuitry for continuous sweat ion analysis. (b) Layout of the flexible electrolyte-gated carbon nanotube field-effect transistor (EG-CNTFET)-based ammonium sensors.

Nevertheless, current integration schemes present limitations that hinder the seamless and reliable connection between the sensing element and the readout circuitry. Traditional fabrication processes, such as wire bonding or flip-chip bonding, may not be compatible with flexible substrates (e.g., because of the high temperatures required), restricting the types of sensors and readout electronics that can be employed. This may lead to challenges such as signal loss, noise, and poor sensor performance [17]. In this work, we have addressed

Corresponding author: Mattia Petrelli (e-mail: mattia.petrelli@unibz.it).
Mattia Petrelli and Ata Golparvar contributed equally to this work.
Associate Editor: R. Dahiya.
Digital Object Identifier 10.1109/LSENS.2023.3274682

this issue from the system perspective. First, we fabricated flexible and planar EG-CNTFETs on a PI substrate, functionalized with an ion-selective membrane, for NH_4^+ detection in the concentration range of 0.1–100 mM. Afterward, we fabricated a fully flexible coin-cell battery-powered readout circuitry by employing a small-sized, i.e., 40 mm × 45 mm PI substrate [see Fig. 1(a)]. To maximize the flexibility of the circuit, particular attention was given to minimizing the complexity of the hardware and the number of components. Later, the proposed fully flexible readout circuitry was first validated by characterizing the EG-CNTFET-based NH_4^+ sensors, and then, benchmarked with a benchtop semiconductor parameter analyzer, which is a "gold standard" reference point. The results showed good sensitivity of the sensors in the physiological range of NH_4^+ in sweat during physical activity, and that the flexible readout circuitry is fully able to replace the bulky benchtop instrumentation, paving the way for the integration of the sensors in wearable platforms.

II. MATERIALS AND METHODS

A. EG-CNTFETs Fabrication and Functionalization

The layout of the EG-CNTFETs consisted of interdigitated electrodes for source and drain and a planar, U-shaped gate electrode [see Fig. 1(b)] [18]. 95% semiconducting CNTs (Merck, catalog number 773735) were employed as active layer. Five devices (N = 5) were fabricated by following the procedure optimized in [19]. The devices were functionalized with an NH_4^+-selective membrane, based on the nonactin ionophore [8]. 10 µL of the membrane cocktail was drop-casted on the active area of the devices (8.85 mm^2), and the devices were stored for 12h at 4° C [8], [15]. They were then stored at room temperature, immersed in a 1 mM NH_4^+ solution in artificial sweat to achieve conditioning of the ion-selective membrane. The artificial sweat was prepared by mixing 8 mM KCl, 30 mM NaCl, 0.084 mM creatinine, 0.17 mM glucose, 0.059 mM uric acid, and 0.01 mM ascorbic acid in deionized (DI) H_2O, with a resistivity of 18.2 MΩcm [9]. Before and after each measurement, the devices were gently washed with fresh artificial sweat.

B. Readout Circuitry Design

As illustrated in the hardware schematic depicted in Fig. 2, the proposed circuitry comprises two main blocks: front-end readout and power management circuitries. During all the phases of the development (i.e., circuit design, choice of commercial components, and layout routing), the focus was on minimizing the number of components, and on placing them in such a fashion that, when bending the PCB, the parts of the board with physical components remained stationary, while the board itself flexed along predefined horizontal and vertical lines. This strategy allowed us to create a flexible circuit without compromising its functionality.

The first stage of the readout block uses a high-speed (90 MHz Gain Bandwidth), low-noise, precision trans-impedance amplifier (OPA380AID, Texas Instruments, USA) to convert the sensed current into voltage and also to bias the EG-CNTFET-based sensor's source. In its feedback loop sits a digital potentiometer (AD5122A, Analog Devices, USA), whose value is set with the microcontroller (BLUENRG-M2SP, STMicroelectronics, Switzerland) connected via an I^2C serial communication bus. Next, the sensed voltage is digitized with a 24-bit low-power analog to digital converter (ADC, ADS1251U, Texas Instruments, USA). The high 19-bit effective resolution is critical to increasing the accuracy of the measurement. The digitized data are continuously fed to the microcontroller via Serial Peripheral

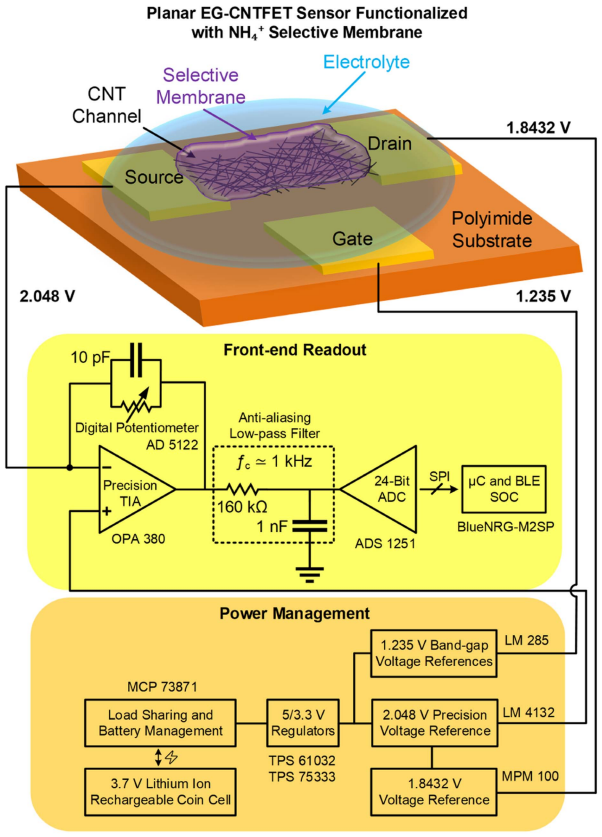

Fig. 2. Schematic representation of the proposed electrolyte-gated ammonium (NH_4^+) sensors, together with the hardware schematic of the flexible circuitry.

Interface (SPI). Finally, the embedded Bluetooth low-energy (BLE) module transmits the sensed information to the custom-designed user interface for the data postprocessing.

The power management block is responsible for charging the 3.7 V lithium-ion coin cell battery, regulating, and generating the required stable bias voltages for the operation of the transistor-based sensor. The battery charge management controller (MCP73871, Microchip Technology, USA) comes with internal load-sharing capability, which enables the charging of the battery while maintaining its operation for a prolonged measurement duration. An efficient (96 %) synchronous boost converter (TPS61032, Texas Instruments, USA) was used to generate the regulated 5 V supply. Regulated 5 V was chosen to be acquired as input to the 3.3 V dc–dc buck down converter instead of the battery's initial 3.7 V (which drops down to ∼3.0 V upon battery usage), to avoid misoperation of the converter. Later, the 5 V is converted to 3.3 V with a low-dropout voltage regular (TPS75333, Texas Instruments, USA) for the micro-controller's operation. Similarly, the regulated 5 V is converted to 2.048 V and 1.235 V to generate reference voltages for biasing the EG-CTNFET-based sensor's source and gate, V_S and V_G, respectively. The gate voltage reference is generated by a band-gap reference connected externally to a 36 kΩ resistor (LM385-1.2, Texas Instruments, USA), since the sensor can tolerate the typical 1% to 2% tolerance of band-gap voltage references in its gate. However, the drain–source voltage is required to be ultrastable to minimize measurement errors due to readout noise. Therefore, a precision voltage reference with an accuracy of sub 1% is implemented to produce the source bias voltage (LM4132, Texas Instruments, USA). Subsequently, a factory-fixed 10:1 resistor divider network with a

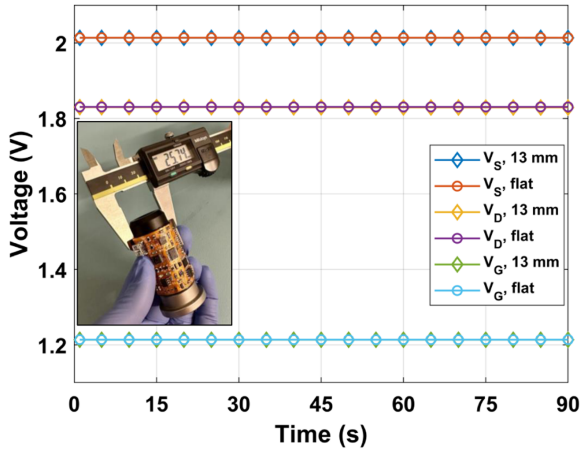

Fig. 3. Bending test performed on the proposed flexible front-end readout circuitry. It can be seen how the output voltages (i.e., V_S, V_D, and V_G), are unaffected by the bending. In the inset, a real picture of the readout circuitry bent around the cylinder used to perform the test.

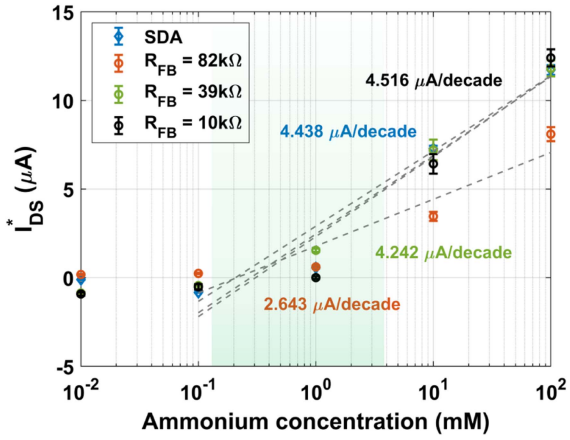

Fig. 4. Corrected response I^*_{DS} of a representative EG-CNTFET-based sensor versus different concentrations of ammonium (NH_4^+), comparing the results obtained with the benchtop semiconductor device parameter analyzer (SDA) with the proposed flexbile readout circuitry, for different values of the feedback resistance R_{FB}. The green box highlights the physiological range of concentrations of NH_4^+ during physical exercise.

tolerance of 0.01 % (MPMT10011002AT5, Vishay Intertechnology, USA) is used to generate the drain bias voltage of 1.8432 V (V_D).

C. Readout Circuitry Validation—EG-CNTFET-Based NH_4^+ Sensors Characterization

To verify the performance of the proposed flexible readout circuitry when flexed, a static bending test was carried out. The circuitry was wrapped around cylinders of different radii (i.e., 13, 20, 28, 35, 50, 80 mm, see the inset of Fig. 3), and the V_G, V_D, and V_S voltages were measured continuously with a digital multimeter (UT161E, Uni-Trend Technology, China) for 90 s.

A semiconductor device parameter analyzer (SDA) (B1500A, Keysight Technologies, USA) was used as a standard reference instrument for the benchmark validation of the proposed custom-designed circuitry. We utilized a standard probe station to interface the flexible sensor with both the custom-designed circuitry and SDA. This approach ensured that any potential nonideality associated with contact and cable connections affected both units equally, thus maintaining comparable recordings for both setups. The drain–source current I_{DS} was recorded in real-time while keeping the biasing fixed at $V_{GS} = -0.81$ V and $V_{DS} = -0.186$ V, to be perfectly in parallel with the voltages applied by the on-board reference voltage employed in the flexible circuitry. Each device was tested with the SDA, and then, with the developed circuitry, with three different values for the digital potentiometer ($R_{FB} = 10\,k\Omega$, $39\,k\Omega$, and $82\,k\Omega$). The source, drain, and gate electrodes were covered with 200 µL of artificial sweat, and the I_{DS} was continuously monitored for 70 min to let the device stabilize [20], [21]. Without interrupting the measurement, the EG-CNTFETs were then tested for the detection of five different NH_4^+ concentrations: 0.01, 0.1, 1, 10, 100 mM. An interval of 10 min was employed between two consecutive additions. At the end of each test, the devices were washed with fresh artificial sweat, and between the different tests, they were stored immersed in the conditioning solution for 24 h.

III. RESULTS AND DISCUSSION

The results of the bending test confirmed how the readout circuitry performances are uninfluenced by the bending of the substrate. The results for the smallest tested bending radius (i.e., 13 mm) are reported in Fig. 3. The voltages produced by the circuitry perfectly overlap between the flat condition and the bent condition. Analogous results were collected for the other bending radii.

To correctly compare the measurements carried out with the proposed flexible circuit with the ones taken from the SDA, we estimated the I_{DS} by

$$|I_{DS}| = \frac{V_{TIA} - V_S}{R_{FB}} \tag{1}$$

where V_{TIA} is the output voltage of the trans-impedance amplifier (TIA) and V_S the voltage at the source electrode of the EG-CNTFET. From (1), it is straightforward that saturation of the TIA can occur increasing the value of R_{FB}. In this respect, the value of R_{FB} sets the tradeoff between sensitivity and the dynamic linear detection range of the measurement (i.e., of the TIA). By taking into account the highest value of R_{FB} tested, i.e., $R_{FB} = 82\,k\Omega$, it could be calculated a theoretical upper limit for the $|I_{DS}|$ of 30 µA. In fact, we observed saturation of the TIA for 4 out of the 5 tested devices, when testing $R_{FB} = 82\,k\Omega$. For $R_{FB} = 39\,k\Omega$ and $R_{FB} = 10\,k\Omega$, such issue was not observed.

The corrected response of one of the tested EG-CNTFET-based biosensors (i.e., $I^*_{DS} = I_{DS}$ after the baseline correction [18]) to the different NH_4^+ concentrations and R_{FB} values is depicted in Fig. 4. For $R_{FB} = 10\,k\Omega$ and $R_{FB} = 39\,k\Omega$, the calibration curves showed very good overlap with the measurement taken with the SDA, hence proving the good operation of the proposed circuitry. As mentioned before, the measurements taken with $R_{FB} = 82\,k\Omega$ suffered from the saturation of the TIA, hence the calibration curve did not show the expected behavior and moved away from the measurement taken with the SDA. For all the different testing conditions, the average values of the sensitivities for the five tested devices are reported in Table 1. All the tested devices showed selective detection in a complex electrolyte such as artificial sweat, demonstrating the robustness of the EG-CNTFET-based sensing platform. The values of sensitivities were obtained from the fitting of the I^*_{DS} over the logarithm of the NH_4^+ concentrations. One of the advantages of the proposed approach resides in its digital readout: with

TABLE 1. EG-CNTFET-Based NH_4^+ Biosensors Parameters, Comparing Different Testing Conditioning Procedures

Test	Avg. Sensitivity [μA/decade]	Sensitivity re-STD [%]	R^2 [%]
SDA	4.851	22.37	94.70
$R_{FB} = 82\,k\Omega$	1.564	68.56	92.19
$R_{FB} = 39\,k\Omega$	3.790	17.42	94.07
$R_{FB} = 10\,k\Omega$	4.376	12.43	93.35

a sufficient amount of calibration curves, the microcontroller can be programmed to associate the electrical reading to the actual concentration through look-up tables or statistical inference. The measurements taken with $R_{FB} = 10\,k\Omega$ proved to be the closest to the ones taken with the SDA, followed by $R_{FB} = 39\,k\Omega$. The difference in the value of the relative standard deviation (re-STD) can be addressed to the fact that the devices were kept stored in artificial sweat between the tests [22], [23].

IV. CONCLUSION

In this letter, we presented the design and validation of a flexible readout circuitry for the characterization of flexible and planar EG-CNTFET-based biosensors for NH_4^+ detection. The biosensors were characterized using artificial sweat (a closed mimic of actual human perspiration) as electrolyte, for the detection of NH_4^+ in the range from 0.01 to 100 mM. This experiment served as a proof-of-concept to test the functionality of the proposed readout circuitry: further characterization of the EG-CNTFET-based NH_4^+ sensors will focus on a narrower range of concentrations, possibly increasing the number of concentrations tested inside the physiological range from 0.12 to 2.17 mM. The functionality of the proposed readout circuitry was tested by means of a bending test, and the functionality of the circuitry proved to be unaffected by the bending of the substrate. Furthermore, the circuitry was validated by benchmarking with a standard benchtop-size instrument. Different values of feedback resistance for the employed trans-impedance amplifier were tested, and the optimal value between them individuated ($R_{FB} = 10\,k\Omega$).

This first working prototype proves the feasibility of a holistic approach, in which sensors and circuitry are fabricated using the same flexible substrate. This will pave the way for their integration into a single substrate, e.g., by directly fabricating the sensor in the back side of the flexible PCB, hence overcoming the challenge of forming flexbile, robusts interconnects between the sensor and its readout. Future work will be focused on the design of a dedicated microfluidics system, to achieve a complete portable system for sweat ion monitoring in real-time on human subjects.

ACKNOWLEDGMENT

The work was supported in part by the Autonomous Province of Bolzano-South Tyrol's European Regional Development Fund (ERDF) Program (project codes EFRE/FESR 1068-Senslab and EFRE/FESR 1127-STEX) and in part by Istituto Italiano di Tecnologia (IIT), as well as internal funding of both the Swiss Federal Institute of Technology Lausanne (EPFL) and the Free University of Bolzano (unibz).

REFERENCES

[1] A. Golparvar, O. Ozturk, and M. K. Yapici, "Gel-free wearable electroencephalography (EEG) with soft graphene textiles," in *Proc. IEEE Sensors*, 2021, pp. 1–4.
[2] O. Ozturk, A. Golparvar, G. Acar, S. Guler, and M. K. Yapici, "Single-arm diagnostic electrocardiography with printed graphene on wearable textiles," *Sensors Actuators A, Phys.*, vol. 349, 2023, Art. no. 114058.
[3] A. Golparvar, A. Boukhayma, M. Petrelli, C. Enz, and S. Carrara, "Optical urea sensing in sweat for kidney healthcare by sensitive and selective non-enhanced raman spectroscopy," *Proc. SPIE*, vol. 12387, pp. 91–97, 2023.
[4] F. Criscuolo et al., "Wearable multifunctional sweat-sensing system for efficient healthcare monitoring," *Sensors Actuators B, Chem.*, vol. 328, 2021, Art. no. 129017.
[5] S. Tonello et al., "Amperometric measurements by a novel aerosol jet printed flexible sensor for wearable applications," *IEEE Trans. Instrum. Meas.*, vol. 72, Nov. 2022, Art no. 7500512, doi: 10.1109/TIM.2022.3225014.
[6] M. Cuartero, N. Colozza, B. M. Fernández-Pérez, and G. A. Crespo, "Why ammonium detection is particularly challenging but insightful with ionophore-based potentiometric sensors—An overview of the progress in the last 20 years," *Analyst*, vol. 145, no. 9, pp. 3188–3210, 2020.
[7] E. Renner, N. Lang, B. Langenstein, M. Struck, and T. Bertsch, "Validating sweat ammonia as physiological parameter for wearable devices in sports science," in *Proc. IEEE 42nd Annu. Int. Conf. Eng. Med. Biol. Soc.*, 2020, pp. 4644–4647.
[8] T. Guinovart, A. J. Bandodkar, J. R. Windmiller, F. J. Andrade, and J. Wang, "A potentiometric tattoo sensor for monitoring ammonium in sweat," *Analyst*, vol. 138, no. 22, pp. 7031–7038, 2013.
[9] A. M. Zamarayeva et al., "Optimization of printed sensors to monitor sodium, ammonium, and lactate in sweat," *APL Mater.*, vol. 8, no. 10, 2020, Art. no. 100905.
[10] S. H. Kim et al., "Electrolyte-gated transistors for organic and printed electronics," *Adv. Mater.*, vol. 25, no. 13, pp. 1822–1846, 2013.
[11] N. Nakatsuka et al., "Aptamer–field-effect transistors overcome Debye length limitations for small-molecule sensing," *Science*, vol. 362, no. 6412, pp. 319–324, 2018.
[12] B. Shkodra et al., "Electrolyte-gated carbon nanotube field-effect transistor-based biosensors: Principles and applications," *Appl. Phys. Rev.*, vol. 8, no. 4, 2021, Art. no. 041325.
[13] G. Elli et al., "Field-effect transistor-based biosensors for environmental and agricultural monitoring," *Sensors*, vol. 22, no. 11, 2022, Art. no. 4178.
[14] B. Shkodra et al., "Flexible carbon nanotube-based electrolyte-gated field-effect transistor for spermidine detection," in *Proc. IEEE Int. Conf. Flexible Printable Sensors Syst.*, 2021, pp. 1–4.
[15] M. Petrelli et al., "From rigid to flexible: Solution-processed carbon nanotube deposition on polymeric substrates for the fabrication of conformal transistor-based ion sensors," *IEEE J. Flexbile Electron.*, to be published.
[16] D. Briand, F. Molina-Lopez, A. V. Quintero, C. Ataman, J. Courbat, and N. F. de Rooij, "Why going towards plastic and flexible sensors?," *Procedia Eng.*, vol. 25, pp. 8–15, 2011.
[17] A. J. Golparvar and M. K. Yapici, "Toward graphene textiles in wearable eye tracking systems for human–machine interaction," *Beilstein J. Nanotechnol.*, vol. 12, no. 1, pp. 180–189, 2021.
[18] M. Petrelli et al., "Novel gate electrode design for flexible planar electrolyte-gated field-effect transistor-based sensors for real-time ammonium detection," in *Proc. IEEE Sensors*, 2022, pp. 1–4.
[19] B. Shkodra, M. Petrelli, M. A. Costa Angeli, A. S. Inam, P. Lugli, and L. Petti, "Optimization of the spray-deposited carbon nanotube semiconducting channel for electrolyte-gated field-effect transistor-based biosensing applications," *IEEE Sensors J.*, early access, Mar. 29, 2022, doi: 10.1109/JSEN.2022.3162706.
[20] M. Petrelli et al., "Flexible, planar, and stable electrolyte-gated carbon nanotube field-effect transistor-based sensor for ammonium detection in sweat," in *Proc. IEEE Int. Flexible Electron. Technol. Conf.*, 2022, pp. 1–2, doi: 10.1109/IFETC53656.2022.9948472.
[21] M. Petrelli et al., "Method for instability compensation and detection of ammonium in sweat via conformal electrolyte-gated field-effect transistors," *Org. Electron., to be published*.
[22] T. Sokalski, A. Ceresa, M. Fibbioli, T. Zwickl, E. Bakker, and E. Pretsch, "Lowering the detection limit of solvent polymeric ion-selective membrane electrodes. 2. influence of composition of sample and internal electrolyte solution," *Anal. Chem.*, vol. 71, no. 6, pp. 1210–1214, 1999.
[23] A. Michalska, K. Pyrzyńska, and K. Maksymiuk, "Method of achieving desired potentiometric responses of polyacrylate-based ion-selective membranes," *Anal. Chem.*, vol. 80, no. 10, pp. 3921–3924, 2008.

Open Access funding provided by 'Libera Università di Bolzano' within the CRUI CARE Agreement